Interaction of Apical and Basal Membrane Ion Channels Underlies Electroreception in Ampullary Epithelia of Skates

Jin Lu and Harvey M. Fishman
Department of Physiology and Biophysics, University of Texas Medical Branch, Galveston, Texas 77555-0641 USA

ABSTRACT The exquisite sensitivity of elasmobranch fishes to electric fields is thought to reside in electroreceptive organs called ampullae of Lorenzini. We measured the stimulus-response behavior of ampullary organs excised from skates. Under open-circuit conditions, the ampullary organ showed three distinct response states: spontaneous repetitive spikes, evoked spikes, and small, damped oscillatory responses. Under short-circuit conditions, the amplitude range for a linear current response to a sinusoidal (0.5 Hz) voltage clamp of an organ (assessed by spectral analysis of the harmonics generated) was 7–200 μV rms. Changes in the spike firing rate of the afferent nerve innervating the organ were evident for voltage clamps of the ampullary epithelium of 3 μV and the spike rate saturated for clamp steps exceeding 100 μV. Thus, the linear response range of the ampullary epithelium exceeded the range in spike firing rate of the afferent nerve. The steady-state transorgan electrical properties under voltage clamp conditions were obtained by analysis of complex admittance determinations in the frequency range 0.05–20 Hz for perturbations (<100 μV rms) in the linear range. Admittance functions were distinctly related to the preparation states observed under open-circuit conditions. A negative real part in the organ admittance (i.e., a steady-state negative conductance generated by the preparation) was a common characteristic of the two (open-circuit) excitable states. The negative conductance was also confirmed by the direction of current flow through the ampullary epithelium in response to step voltage clamps. We conclude that the steady state-negative conductance is an essential property of the ampullary epithelium, and we suggest that the interplay of negative and positive conductances generated by ion channels in apical and basal membranes of receptor cells results in signal amplification that may contribute significantly to the electric field sensitivity of ampullary organs.

INTRODUCTION

The macroscopic electrophysiology of the ampullary organ in elasmobranch fishes was characterized more than 15 years ago after establishment of its primary role in electroreception (Waltman, 1966; Murray, 1962, 1967; Obara and Bennett, 1972; Clusin and Bennett 1977a, b, 1979; Kalmijn, 1982). After a series of studies, Bennett and Clusin (1978) proposed a hypothesis of electroreceptor function in which oscillations and spike activity in the apical membrane of ampullary receptor cells play a crucial role. The oscillations are thought to synchronize individual electroreceptor cells in response to stimuli, and spike activity is thought to reflect the maintenance of a threshold membrane potential at which sensitivity is maximized.

A second hypothesis by Broun and Govardovskii (1983a, b, 1984) prompted a different interpretation. They showed how an assumed N-shaped current-voltage I(V) characteristic in the apical membrane of receptor cells could explain ampullary responses to stimuli. Although Bennett and Clusin reported that the receptor epithelium operated in a negative slope region of the I(V) curve, this observation did not have a significant role in their hypothesis. Broun and Govardovskii attributed the high sensitivity of ampullae to special properties of the synapses at the basal membranes of receptor cells. Further, according to Broun and Govardovskii, the spikes observed by Clusin and Bennett (1977a) were the result of stimulation amplitudes (>50 nA), well beyond the operational range of ampullae. Consequently, these two groups placed different emphasis on the properties of an ampulla that are prerequisite for understanding ampullary function.

The present study was initiated to provide the information from which a resolution of apparent differences between the two groups could be made. We used harmonic analysis to determine the amplitude range over which the current through an ampullary organ responds linearly to voltage clamp stimuli. Then we determined the organ transfer characteristic, i.e., the dependence of afferent nerve output (spike frequency) on transampullary voltage. Finally, we examined the ampullary organ electrical properties by measurement and analysis of driving-point functions in the frequency domain (complex impedance or admittance; Fishman, 1992). Based on our experimental results, the essential property of the ampullary epithelium is the generation of a steady-state negative conductance, which Bennett and Clusin also reported and Broun and Govardovskii had assumed. From our measurements, we infer that the steady-state negative conductance is generated by ion channels in apical membranes of receptor cells and a steady-state positive conductance is characteristic of basal membrane ion conduction. Further, we show how the interplay between the negative and positive conductances can provide amplification of stimuli in the first stage of signal processing. We conclude then that the ampullary epithelium functions as a linear amplifier within its operational range ($\leq$100 μV).

Received for publication 27 April 1994 and in final form 19 July 1994.
Address reprint requests to Dr. Harvey M. Fishman, Department of Physiology and Biophysics, University of Texas Medical Branch, Galveston, TX 77555-0641. Tel.: 409-772-1826; Fax: 409-772-3381.

0006-3495/94/10/1525/09 $2.00

MATERIALS AND METHODS

Preparation and solutions

A preparation consisted of an isolated whole organ: a 3-cm length of canal with ampulla that was innervated by a 5-mm length of afferent nerve. Organs were excised from live, anesthetized skates (*Raja erinacea, Raja ocellata*) at the Marine Biological Laboratory in Woods Hole, MA. Several organs were removed simultaneously as a group, from one side of an animal. Solutions were prepared, and experiments were carried out at room temperature (20–22°C). The group of organs was placed in Elasmobranch saline (in mM: 415 urea, 340 NaCl, 6 KCl, 1.8 $CaCl_2$, 2.5 $MgCl_2$, 2.5 $NaHCO_3$, and 5 HEPES buffer, pH adjusted to 7.4) in a covered petri dish on a cold plate. Individual organs were dissected, as required, without noticeable deterioration of the group over the course of 4–6 h. Preparation cooling before usage did not affect the results.

Two solution-filled chambers, similar to that described previously (Clusin and Bennett, 1977a), separated by an air gap were used for stimulating and recording transorgan responses (Fig. 1). The portion of canal between the two chambers was suspended in air and was washed initially with deionized 0.8 M sucrose solution. The ampulla with attached nerve was placed in one chamber and bathed in Elasmobranch saline. The other cut end of the canal was placed in the second chamber, which was filled with artificial sea water (ASW in mM: 428 NaCl, 13 KCl, 10 $CaCl_2$, 50 $MgCl_2$, 75 urea, 5 HEPES, pH adjusted to 8.1). Afferent nerve responses were recorded by a saline-filled glass pipette with inserted Ag-AgCl electrode after sucking the nerve bundle (5–7 units) of an ampulla into the pipette and lifting the nerve into air.

Electrodes and voltage clamp

A pair of chlorided-silver pellet electrodes (each having an impedance of 400 Ω or less over the frequency range of measurements) in each chamber was used to apply current or voltage stimuli to the organ. These electrodes were also used to record the corresponding transorgan voltage or current response without significant effects caused by current electrode polarization (see Fig. 1). Constant current stimuli were delivered by a Howland current pump. Voltage control of the organ was attained by use of an epithelial voltage clamp system (Fishman and Macey, 1969) connected to the chlorided-silver pellet electrodes. Voltage clamp of the ampullary epithelium was implemented by substitution of the measured transampullary voltage for the transorgan voltage in the clamp system. The transampullary voltage was obtained from a long, tapered electrolyte-filled pipette by placement of its tip near the lumenal surface of the ampulla.

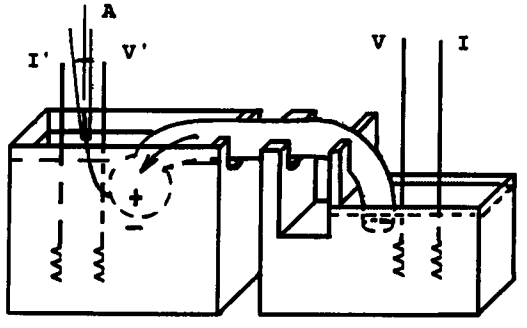

FIGURE 1 Diagram of an isolated organ preparation with electrodes for stimulus/response measurements. *I'* is a virtual ground point used to measure currents through an ampullary organ; *V–V'* are used to measure transorgan potentials; *I* is a current-passing electrode for current-clamping the preparation from a constant current source or in voltage clamp mode is connected to the output of the control amplifier. See text for description of transampullary voltage clamp. Label *A* is afferent nerve fiber potential, measured with respect to ground. Current flow in the direction of the arrow is a lumenal positive stimulus that inhibits nerve activity.

Conventional use of "depolarization" and "hyperpolarization"

The terms "depolarization" and "hyperpolarization" are defined as polarizations measured across the ampullary epithelium (basal side as the reference) that result in an increase (excitatory) and a decrease (inhibitory), respectively, in the spike firing rate of the afferent nerve innervating the ampulla. An applied current directed out of a canal (i.e., flowing across the ampullary epithelium from basal to lumenal surfaces) produces excitatory discharges in the afferent nerve and a negative lumenal potential. Thus, stimuli that make the lumen more negative are designated depolarizing, and stimuli that make the lumen more positive are designated hyperpolarizing.

Assessment of the linearity of the transorgan response by harmonic analysis

The response of a linear system to a sinusoidal stimulus of a particular frequency is another sinusoid of the same frequency differing only in amplitude and phase. When the total harmonic content of the response (used as a measure of the degree of nonlinearity) was <1% of the fundamental, we considered the system to be linear (Moore et al., 1980). Under voltage clamp conditions, the fundamental and harmonic components of the current in response to a 0.5 Hz sinusoidal voltage stimulus of various amplitudes applied across the organ were determined by spectral analysis (Rockland Instruments, Model 512/s FFT Analyzer).

Driving-point function determinations

To characterize the transorgan conduction properties, we used complex admittance spectroscopy (Fishman, 1992). The time course of the current, $I_{TO}(t)$, through an organ was obtained in response to a small amplitude, synthesized waveform (<100 μV rms), consisting of the sum of 400 sinusoids from 0.05 to 20 Hz, applied as a repetitive (waveform period of 20 s) transorgan voltage, $V_{TO}(t)$. Data were acquired in a steady state (after one or more cycles of the synthesized signal had occurred). The total experimental time to acquire a single response took about 2 min. The complex admittance, $Y_{TO}(jf)$, of the organ was computed as

$$Y_{TO}(jf) = \frac{\mathcal{F}[I_{TO}(t)]}{\mathcal{F}[V_{TO}(t)]} = \frac{I_{TO}(jf)}{V_{TO}(jf)} = G(f) + jB(f), \quad (1)$$

where $\mathcal{F}$ denotes a fast Fourier transform of the sampled functions of time $I_{TO}(t)$ and $V_{TO}(t)$, and $I_{TO}(jf)$ and $V_{TO}(jf)$ are the transformed functions of complex ($j = (-1)^{1/2}$) frequency (f). In Eq. 1, $G(f)$ is the *real part* and $B(f)$ is the *imaginary part* of $Y_{TO}(jf)$. Admittance data are presented as plots of *imaginary part* versus *real part*.

Admittance modeling

Admittance data were fitted by a model based on the linearized Hodgkin-Huxley equations (Cole, 1968; Mauro et al., 1970) and generalized to the ampullary organ. The admittance model is

$$\frac{1}{Y_{TO}(jf)} = \frac{1}{g_c} + \frac{1}{Y(jf)}. \quad (2)$$

g_c is the canal conductance dominated by the conducting jelly that fills the canal, which consists of relatively nonconducting epithelium (Waltman, 1966), and $Y(jf)$ is the ampullary (transepithelial) admittance given by

$$Y(jf) = j2\pi fC + g + Y_1(jf) \quad (3)$$

$$Y_1(jf) = \frac{g_1}{1 + j2\pi f\tau_1}; \qquad L = \frac{\tau_1}{g_1}, \quad (4)$$

where C is the transampullary capacitance, g is the transampullary "infinite-frequency" conductance, and g_1 is a transampullary conductance that relaxes with characteristic time τ_1 in response to voltage changes across the ampulla. By analogy to an electrical inductance, L reflects an inductive-like susceptance associated with the relaxation kinetics of the transampullary conductance. Curve fits of the model were made by use of software described previously (Fishman and Lipicky, 1991), in which the mean square error between *real* and *imaginary* parts of the model and data at all frequencies was minimized to obtain model parameter estimates for the best fit. The mean square error is $\langle(G(f) - G_M(f))\rangle^2 + \langle(B(f) - B_M(f))\rangle^2$, where $G(f)$ and $B(f)$ are data obtained by use of Eq. 1, and $G_M(f)$ and $B_M(f)$ are the *real* and *imaginary* parts of the model admittance (Eq. 2), respectively.

Transfer characteristic determinations

To obtain the relationship between a voltage-clamped ampulla at the μV level and its afferent nerve firing rate, we took advantage of the short-term (min) DC stability of electrodes and used short duration (0.5 s) pulses. The pulse duration of 0.5 s was chosen to avoid postsynaptic adaptation, which reduces firing rate to one-half its initial value in 3–5 s (Murray, 1974). The short-term (min) DC stability of all electrodes used for these experiments was measured to be no worse than 4 μV in a 5-min interval. To further minimize effects caused by electrode drift, the resting (reference) firing rate was determined in the 0.5-s interval immediately before application of each pulse. The relative firing rate was then computed as the ratio of the rate during the pulse to the rate before the pulse. Under these conditions, the relative firing rate was found to be reproducible for the same amplitude (3 μV or more) pulse applied at different times.

RESULTS

Open-circuit ampullary states

Under the conditions depicted in Fig. 1, the transorgan resting potential of the isolated ampulla ranged between −0.1 and −4.0 mV (basal side reference). Based on our measurements of the transorgan voltage, V_{TO} (voltage between V and V'), under current clamp conditions in more than 100 preparations, ampullae exhibited one of three response states. In State I, spontaneous repetitive spikes occurred (Fig. 2 *A*). In this state, V_{TO} showed spontaneous, repetitive spikes (20–40 mV) at frequencies between 0.5 and 0.75 Hz. In State II, generation of all-or-nothing spikes (up to 80 mV amplitude) required a lumen negative (depolarizing) current stimulus ≥0.6 nA (Fig. 2 *B*). In the third state (III), a small (<1 mV) oscillatory response (damped ringing) was seen in V_{TO} when a stimulus was applied to the preparation (Fig. 2 *C*). Spikes in V_{TO} could not be evoked in this state for stimulating currents up to 150 nA.

The total resistance of the preparation was also indicative of the state of the preparation. We used relatively large current pulses (5–10 nA) to assess the preparation resistance that yielded values for the ampullary organ resistance that ranged from 80 kΩ to 5 MΩ. The mean resistance of the ampullary organ in State I was always highest (977 ± 346 kΩ; SEM), ranging from 400 kΩ to 5 MΩ. The resistance in this state (determined in six preparations) was the most variable (Table 1). The mean resistance of an ampullary organ in State II was high (322 ± 72 kΩ; SEM), but always less than that found in State I. The mean resistance of State III was invariably the lowest (162 ± 28 kΩ; SEM). High resistance usually is indicative of a physiologically relevant condition of a preparation. Furthermore, freshly dissected ampullary organs from healthy, live animals usually existed in State I or State II (95/110 preparations). State III most often occurred at the end of experiments. Freshly dissected preparations were found in State III only when the organ was damaged. Therefore, we concluded that State III was indicative of a deteriorating preparation.

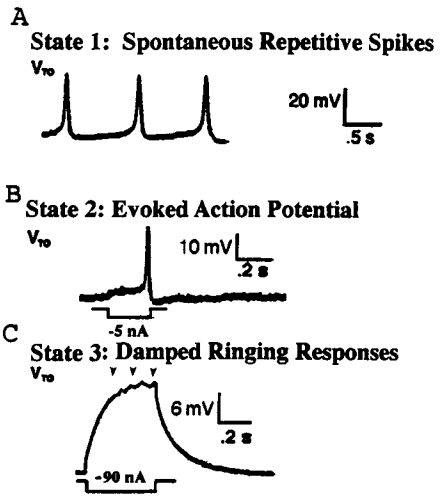

FIGURE 2 Three distinct open-circuit response states in isolated organ preparations. Trans-organ voltage, V_{TO} (voltage between V and V') is as in Fig. 1. Downward current pulse indicates negative polarization of lumenal potential. (*A*) State I: Spontaneous repetitive spikes. (*B*) State II: Evoked spikes. (*C*) State III: Damped ringing responses.

TABLE 1 Resistance Measurement (n = 6)

State I (kΩ)	State II (kΩ)	State III (kΩ)
977 ± 346	322 ± 72	162 ± 28

Note: Values are mean ± SEM.

All states were stable lasting from minutes to hours. Transitions between states (I and II) occurred often but spontaneously rather than regularly. Fig. 4 *C* shows an example of such a transition of transorgan potential from State I to State II. An ampulla could also be forced to make a transition from State II to State I by application of current stimuli >5 nA. Once a preparation entered State III, it did not recover to State I or II. In a few rare cases, the ampulla initially exhibited State III behavior, but then made a transition to State I or II, indicating some recovery from trauma.

We also studied transorgan responses to current stimuli while the preparation was in State I. Repetitive spike discharges in the ampullary epithelium decreased as holding current hyperpolarized the preparation. Thus, the spike firing rate of the ampullary epithelium could be tuned by varying the amplitude of the holding current (Fig. 3 *A*). The steady-state firing rate of three preparations from different skates is shown in Fig. 3 *B*. These ampullary epithelial phenomena were also reflected in afferent nerve activity (see next section).

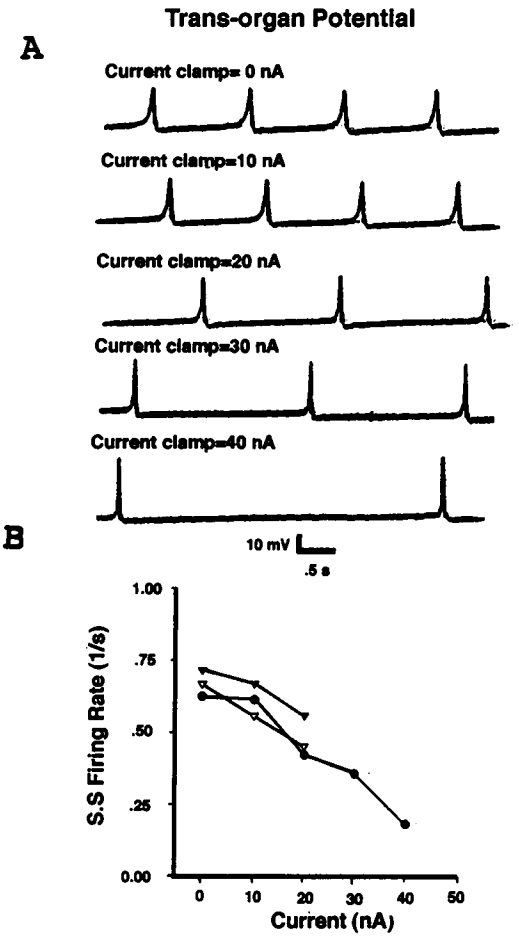

FIGURE 3 (*A*) Alteration of transorgan (ampullary epithelium) spike firing rate with applied constant current. (*B*) Plot of steady-state firing rate versus constant current level.

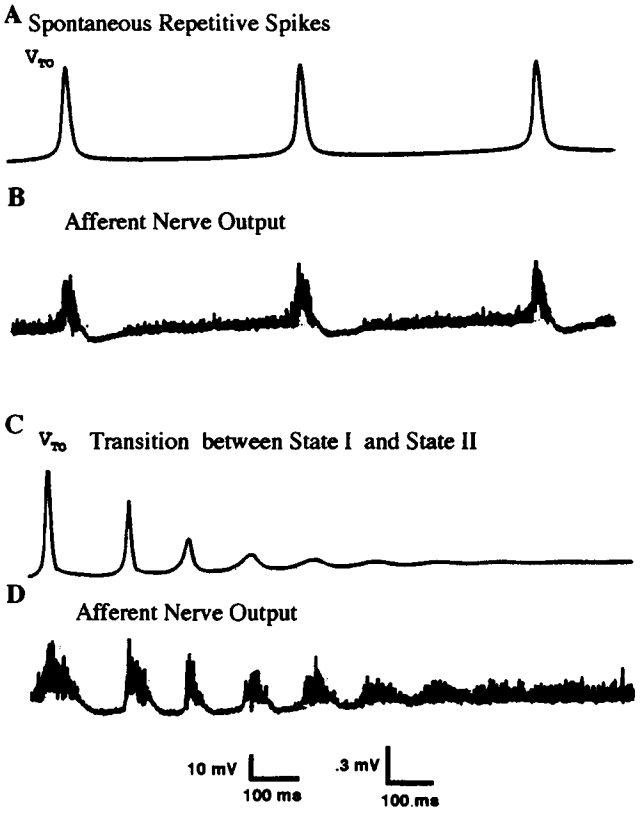

FIGURE 4 The relationship between transorgan (transampullary) voltage and afferent nerve activity under current clamp condition with no stimulus applied. (*A*) V_{TO} in State I. (*B*) Afferent nerve output showing postsynaptic potentials and tonic activity reflecting the pattern of transorgan potential. (*C*) V_{TO} reflecting the transition between State I and State II. (*D*) Afferent nerve activity corresponding to the transition between states shown in *C*.

Transfer characteristic of ampullary epithelium to afferent nerve

We found that activity in the nerve innervating the basal membrane of receptor cells of the ampullary epithelium reflected transorgan potential changes directly. Without an applied stimulus to the ampullary epithelium, afferent nerve activity was tonic at about 30–40 spikes/s. This resting spike rate is in the range of single unit recordings from afferent nerve in situ on skates (Murray, 1962). However, Murray dissected the nerve to obtain only a few active units. The similarity between our resting spike rates and those of Murray suggests that our recordings were also from a few units. Fig. 4 *A* shows that postsynaptic potentials (PSPs) recorded from isolated, whole afferent nerve were synchronous with the occurrence of spikes during spontaneous repetitive activity in V_{TO}. In addition, resting, tonic spike-firing rate accelerated in nerve during the rising phase of spikes in V_{TO} and decelerated during the falling phase in V_{TO} until nerve spike discharge came to a complete halt at the "foot" of each ampullary spike. As V_{TO} stabilized during the next 100 ms, nerve spike activity continued to be inhibited. Subsequently and before the occurrence of the next spike in V_{TO}, resting tonic nerve discharge returned. Transitions between States I and II were also reflected directly in afferent nerve PSPs and spike discharge rate (Fig. 4, *C* and *D*). Therefore, the afferent nerve fibers indeed convey information about the transampullary epithelial voltage to the central nervous system by means of the afferent spike discharge rate.

The signal transfer characteristic from ampullary epithelium to afferent nerve was also determined (Fig. 5). During voltage clamps of receptor epithelium, the ampullary firing rate of the nerve showed inhibitory and excitatory responses to positive and negative lumen potentials (≥ 3 μV, $n = 3$), respectively. The sensitivity of an ampulla to electrical fields also was reflected in the very high slope of the transfer curve (3.7% of nerve firing rate at rest/μV). The nerve impulse generation rate saturated for stimuli above 100 μV ($n = 3$), which is indicative of the upper limit of the operational range of the afferent nerve.

Short-circuit of ampullary organ

Under voltage clamp conditions, the steady-state current through an ampullary organ was in the opposite direction to that expected for a positive conductance in response to a small step voltage stimulus. Fig. 6 *A* shows that ampullary

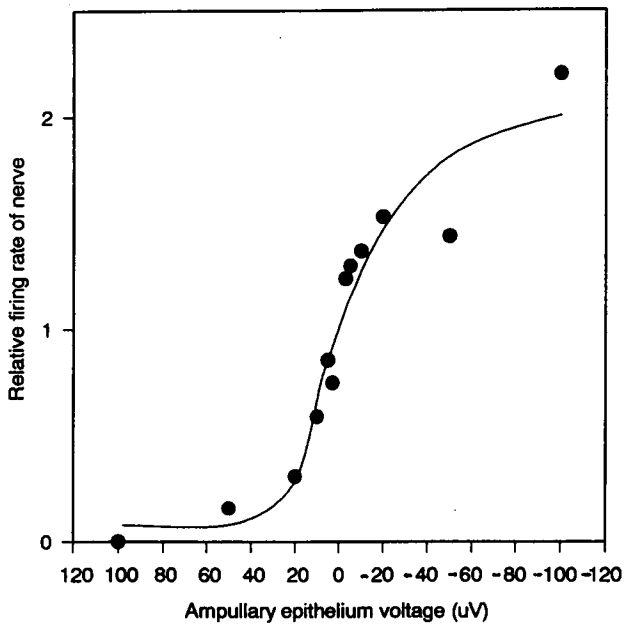

FIGURE 5 Transfer characteristic curve of an ampullary organ. Data were obtained by determining the firing rate of the afferent nerve relative to the resting firing rate in response to transepithelial voltage clamps from 0 mV holding potential. Solid line is a curve fit of a logistic function to the data. The slope of the curve at 0 mV is 1.05 Hz/μV. Note that ampullary epithelium voltage <0 (i.e., lumen negative) increases afferent nerve activity and, therefore, is excitatory.

currents were directed from basal to apical membrane of receptor cells (a downward deflection) in response to small pulses (lumenal positive) applied to the voltage-clamped ampullary organ. The amplitude of the current reached a steady-state level immediately after an early capacitive current transient. This steady current, directed out of the open end of the canal of the preparation, showed no obvious inactivation and was quite stable. With increasing voltage stimuli, the current responses first increased and then gradually decreased (see the responses of stimuli for 8 and 15 mV). The "tail current" response after the return of the clamp voltage to the holding potential showed overshoot and ringing for progressively larger clamp pulses. This ringing in the "tail current" response suggests that strong stimuli (mV) can drive the preparation from State I or II into State III.

Fig. 6 *B* shows that under different holding potentials (HP), the preparation exhibited more or less steady-state negative slopes in response to voltage pulses less than 4 mV. Preparations responded with increased negative current to increasingly negative lumenal holding potentials. The largest current often occurred in response to a 4–8 mV voltage stimulus. For voltage steps exceeding 8 mV, the preparation current showed a steady-state positive slope relationship.

Linearity in harmonic measurements under voltage clamp conditions

Use of complex admittance determinations to describe preparation behavior requires that responses to changes in driving-

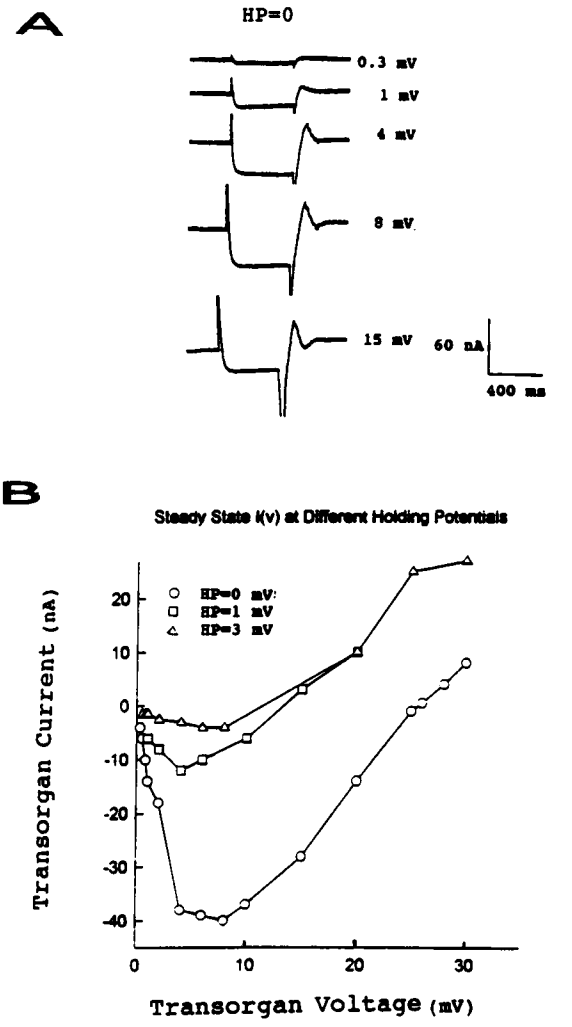

FIGURE 6 Step voltage clamp data from an ampullary organ. (*A*) The indicate voltages beside each trace are lumen-positive clamp steps from a transorgan holding potential (HP) of 0 mV relative to the basal side of receptor cells. A Downward (negative) deflection represents current directed from basal to lumenal membrane. (*B*) The preparation steady current response to voltage clamp steps from the different HPs. The current direction defined in *A* also applies to *B*.

function amplitude be proportionate (linear). The linear response range of a preparation is also an important attribute of preparation behavior. Harmonic generation is one of the simplest ways to determine the linear range of ampullary responses. For 0.5 Hz sinusoidal voltage stimuli, preparations gave linear responses (the rms value of all harmonics was <1% of the rms value of the fundamental) in the range of 7–200 μV rms (see Fig. 7 for data from 1 of 9 preparations used for harmonic analysis). Significant nonlinearity (harmonic content of 10% or more) was observed for stimuli in excess of 500 μV rms. In summary, within the voltage range (<200 μV) of ampullae, we found that the ampullary organ not only operates on the negative slope of its I(V) curve, but also operates linearly. Considering the operational range of the afferent nerve (Fig. 5) and the ampullary epithelium, an isolated ampullary organ functions at stimulus voltages below 100 μV.

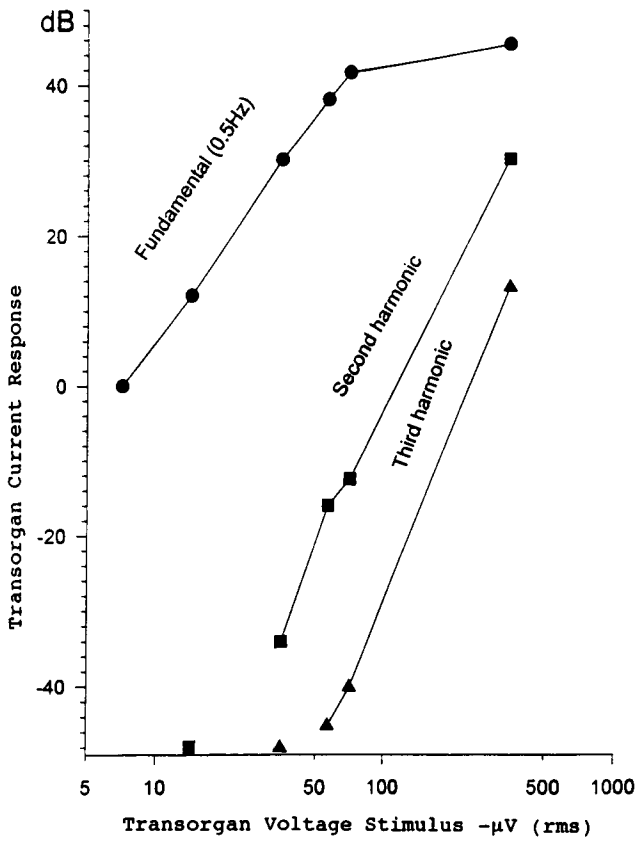

FIGURE 7 Harmonics generated by a voltage-clamped ampullary organ at a holding potential of 0 mV. Transorgan current was recorded in response to various amplitudes of 0.5 Hz sinusoidal voltage superposed on the holding potential. The generation of significant harmonics (2nd and 3rd) relative to the amplitude of the fundamental (0.5 Hz) is indicative of nonlinearity, which became significant (10% of fundamental) above 500 μV. The total harmonic content for this organ was <1% for stimuli <100 μV rms.

Three distinct admittance functions correspond to the three states observed in current clamp

In the current clamp (open-circuit) condition, we found that the transorgan potential existed in one of three states (spontaneous repetitive spikes, all-or-nothing evoked spikes, and damped oscillations). Under voltage clamp (short-circuit) of the whole ampullary organ, we also observed three distinct characteristics of the ampullary organ in admittance measurements, which corresponded to the three response states observed under open-circuit conditions. Fig. 8 shows the locus of 400 data points (*dots*) plotted in the complex plane [($B(f)$ vs. $G(f)$)], in the frequency range from 0.05 to 20 Hz. The salient feature of the admittance of the preparation in Fig. 8 *A* is that the low frequency (<20 Hz) locus is in the left half plane. Thus, the *real part* of $Y_{TO}(jf)$ (Eq. 1) is negative, and the low frequency behavior of the preparation, in the steady state, is described by a negative conductance. Another significant feature of the admittance locus is that the low frequency data (<2 Hz) have a negative *imaginary part*. The locus also intercepts the *real* axis (i.e., the *imaginary part* is zero) at 2.1 Hz, and at this frequency the admittance reflects solely a negative conductance. These organ admittance characteristics correspond to State I, observed in current clamp mode, because they were present whenever we switched the preparation to voltage clamp mode after observing State I in current clamp mode and vice versa. The distinguishing character of the admittance locus of the preparation in Fig. 8 *B*, corresponding to State II, is that the *real part* of $Y_{TO}(jf)$ is negative but the *imaginary part* is positive at all frequencies in the band, i.e., the locus does not cross the *real* axis. The admittance of the preparation in this state could be driven to the admittance corresponding to State I by

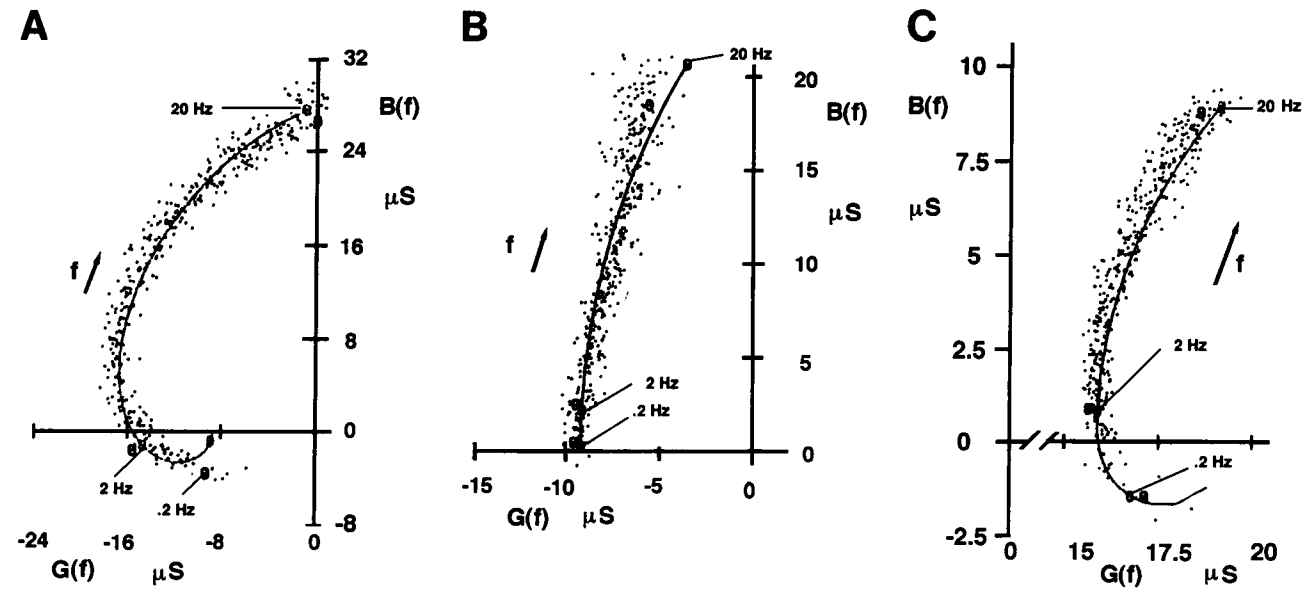

FIGURE 8 Complex admittance of an organ preparation under voltage clamp conditions. The dots are data; solid lines are best fits (minimization of mean square error) of the model in Fig. 9 to the data. *A* corresponds to open-circuit State I. *B* corresponds to open-circuit State II. *C* corresponds to open-circuit State III. In *A*, *B*, and *C*, voltage clamp of V_{To} to 0 mV with superposed voltage stimulus (synthesized signal) of 16 μV ms for admittance determination.

increasing the stimulus amplitude. This observation in voltage clamp was similar to the one in current clamp in which the preparation could be driven from State II to I by increasing stimulus amplitude.

Fig. 8 *C* shows an example of the admittance corresponding to State III. The distinctive characteristic of this state in voltage clamp is that the *real part* of $Y_{TO}(jf)$ is positive, and the *imaginary part* of $Y_{TO}(jf)$ is negative at low frequencies.

Model fitting

To obtain a quantitative description of the admittance at rest, Eqs. 4 and 5 were fitted to the data obtained at the various clamp voltages. The best fits of these equations allowing all quantities to be variable in the fitting process are shown in Fig. 8 (*solid curves*). A circuit realization of the model is shown in Fig. 9. The model parameter estimates obtained from the best fits of admittance data corresponding to each state are listed in Table 2. The conductance g in the model (Eq. 3) was assumed to consist of the sum of a positive (g_+) and a negative (g_-) conductance as defined below.

$$g = g_- + g_+ \tag{5}$$

R_E and R_{net} are zero-frequency resistances of the ampullary epithelium [$R_E = 1/(g_1 + g)$] and of the organ [$R_{net} = (1/g_c) + R_E$], respectively. Other parameters are defined in the admittance modeling section of Materials and Methods. Based on best fits of admittance measurements of nine different preparations, membrane capacitance was relatively constant in all states. Canal resistance estimates were also nearly invariant. R_E in State I, II, and III was -137, -124, and 29 kΩ, respectively. The major difference between State I and II is that State I has an inductive-like susceptance with time constant of 114 ms and State II showed drastically reduced inductive-like susceptance with a time constant of 4 ms (see Eq. 4). The salient property of the preparation in State III was its net positive conductance character. The circuit in Fig. 9 is thus the simplest representation of the transorgan admittance that can fit the admittance data obtained in these experiments.

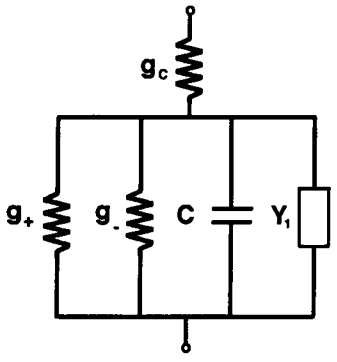

FIGURE 9 A circuit representation of trans-organ conductance model. g_c stands for canal conductance, g_+ and g_- are ampullary positive and negative conductances, respectively, C is epithelial capacitance, and $Y_1(jf)$ branch stands for the relaxing conductance in the ampullary epithelium.

DISCUSSION

Ampulla transepithelial response characteristics

The main observations in our open-circuit and short-circuit preparation experiments are summarized as follows:

1. State I (Fig. 2 *A*) was characterized by a regularly occurring stable behavior in over 60 isolated preparations which remained active from minutes to hours. Preparations made irregular transitions between State I and State II and back again for several hours. The preparation had the highest resistance while in State I, and this state may be physiologically relevant.

2. State II behavior was similar to that reported by Clusin and Bennett (1977a). We also observed this state frequently. However, Bennett and Clusin (1978) found that currents of 50–100 nA were required to elicit ampullary spikes, whereas we could elicit spikes with current pulses (0.6–10 nA) more than 10-fold less (Fig. 2 *B*). The lower current threshold may be because of the difference in observed resting transampullary potential. Bennett and Clusin (1978) reported resting potentials of 20–30 mV. However, we observed resting potentials no larger than 4 mV, which is closer to 2 mV or less observed by Broun and Govaerdovskii (1983a) in *Raja clavata*. A preparation resting, offset voltage of 16 mV or more, for whatever reason, could require substantially more current to reach threshold.

3. State III was marked by oscillatory and damped ringing responses. Our finding that this type of behavior only occurred after States I or II or in damaged preparations with the lowest resistances suggests that this state is characteristic of a deteriorating preparation.

4. The transampullary response was quite linear for low level voltage clamp stimuli (7–200 μV rms). In this range, the resistance of the preparation was negative. During open-circuit conditions (current clamp), the preparation showed positive resistances for hyperpolarizing stimuli (up to 150 nA), which is also reflected in Fig. 6 *B* (positive slope region of the curve). Because of the shunting effect on each organ of the relatively low resistance pathway through the sea water and the skin of elasmobranchs (Murray, 1967) to the capsule within which ampullae are contained, isolated ampullary organ responses under current clamp conditions (open-circuit) may not reflect the functional behavior of organs in intact animals in sea water.

5. Under short-circuit conditions, the transorgan admittance showed three distinct characteristics that correspond to the three states in current clamp conditions. Admittances corresponding to States I and II showed a steady-state negative conductance, but State I showed inductive-like susceptance, whereas State II did not. State III showed only a positive conductance and negative susceptance, indicative of a

TABLE 2 Parameter estimates from curve fits of admittance in the three states

State	C	R_c	R	R_1	R_2	R_{net}	τ_1
	(μF)	(kΩ)	(kΩ)	(kΩ)	(kΩ)	(kΩ)	(ms)
I	0.15	23	−78	181	−137	−114	114
II	0.14	16	−91	342	−124	−108	4
III	0.20	23	40	101	29	52	1500

damped resonant circuit that would give ringing responses for current clamps.

Ampullary organ transfer characteristics

Previous measurements of the minimum detectable change in afferent nerve activity in response to electric fields (1 μV/cm) applied to *intact animals* showed responses corresponding to μV changes in transampullary voltage (Murray, 1962, 1974). Although this response level of the organ is still a little more than an order of magnitude greater than that obtained from behavioral responses (Kalmijn, 1966, 1982) (10 nV/cm over a 10 cm length canal yields an epithelial voltage drop of 0.1 μV), it nevertheless is several orders more sensitive than most other synapses. Our data now indicate that μV sensitivity is a property of an *isolated organ preparation*. Further, we find that the afferent nerve firing rate saturates for epithelial voltages that exceed 100 μV which, together with our harmonic analysis, suggests that the ampullary epithelium behaves as a linear transducer over the operating range of the afferent nerve.

Negative conductance in ampullary organ admittance

The ampullary electrical behavior can be explained simply (illustrated in Fig. 9) as the interaction of a negative conductance ($g_- < 0$), a positive conductance ($g_+ > 0$), a capacitance (C), and a $Y_1(jf)$ branch. The total admittance is given in Eq. 2. Data were fitted by an admittance model (Eqs. 2–4) represented by the circuit in Fig. 9. $Y_{TO}(jf)$, corresponding to open-circuit State I showed negative *real* and *imaginary* parts at low frequencies. In this case, the negative conductance (g_-) and the inductive (L) part of $Y_1(jf)$ are dominant; the positive conductance (g_+) was comparatively negligible. Admittance loci, corresponding to open-circuit State II, indicated that the negative conductance (g_-) and capacitance (C) elements of the model are dominant and that the other elements are negligible. In loci, corresponding to open-circuit State III, the positive conductance (g_+) is dominant and the data points shifted to the right half plane. The admittance of this simple circuit adequately accounts for the three distinctive admittance characteristics of preparations under short-circuit conditions.

A negative conductance is generated by all excitable membranes and is usually caused by the presence of either or both Na and Ca channels. Ca channels in the apical membrane of receptor cells have been reported previously (Clusin and Bennett, 1977a). A negative conductance arises if the voltage dependence of the open probability of the channels in the membrane (i.e., the voltage dependence of the ionic conductance) is such that the membrane conductance increases when the membrane voltage approaches the magnitude of and is of the same polarity as the Nernst potential for the permeant ion of the channel. Thus, for a negative conductance the current flows in the direction of potential rise instead of in the direction of the drop. Thus, ion channel production of a negative conductance in the ampullary epithelium is the type of mechanism that can satisfy Murray's (1974) assertion that "only in the ampullae does a cathode above the receptor epithelium excite, and this is the polarity which would, by itself, result in hyperpolarization of the membrane at the base of the receptor cells, so whatever mechanism accounts for the greater sensitivity should also account for this reversal."

Amplification by the interplay of apical negative conductance and basal positive conductance

The circuit representation in Fig. 9 lumps the electrical properties of the entire ampullary epithelium into a parallel element circuit. To illustrate the amplification mechanism underlying these observations, we consider the membrane resistance portion of the circuit model (Fig. 10) to be composed of two resistances in series: R_a (apical resistance) and R_b (basal resistance). V_b is the voltage across the basal membrane, V_A is the transepithelial voltage and V_c is the voltage across the ampullary

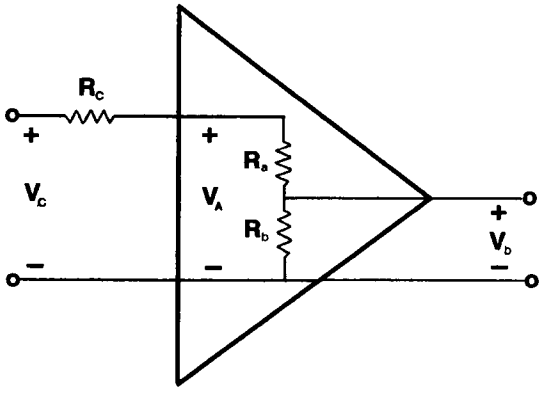

FIGURE 10 A circuit representation that accounts for separate membrane surfaces of receptor cells in the ampullary epithelium. R_a, R_b, and R_c are apical, basal, and canal resistances, respectively. V_c, V_A, and V_b are voltages across the ampullary organ, receptor, and the basal membrane, respectively. Input signal, V_c, can be amplified to produce an output, V_b, affecting neurotransmitter release to the postsynaptic afferent nerve because $R_a < 0$ and $R_b > 0$ (see Eq. 6).

organ. Then V_b is

$$V_b = V_c \cdot \frac{R_b}{R_a + R_b + R_c}. \quad (6)$$

Our data show that a preparation in steady state has a net negative conductance under voltage clamp conditions (Figs. 6 and 8). The canal resistance R_c (Fig. 10), dominated by the conducting jelly, is a positive conductance. Thus, the negative conductance must be generated by the ampullary epithelium. Because a lumenal negative stimulus ($V_c < 0$) causes excitation of the afferent nerve (Fig. 5), the basal membrane must be depolarized (for neurotransmitter release) and V_b is positive. According to Eq. 6, to satisfy all these facts ($V_c < 0$, $V_b > 0$, $R_a + R_b + R_c < 0$), R_b must be positive. The same logic applies for a lumenal positive stimulus, but the result is inhibition of nerve activity. Hence, $V_b < 0$ and, to satisfy all the conditions, our conclusion again is that R_b must be positive. Furthermore, R_a must be negative because our admittance data and step clamp data from a short-circuit organ showed that the total resistance ($R_a + R_b + R_c$) of an organ is negative.

The incremental voltage that is developed across the basal membrane of ampullary receptor cells by virtue of its effect on neurotransmitter release becomes the input to the afferent nerve. The interplay between the negative resistance of R_a (presumably generated by ion channels in the apical membrane) and the positive resistance of R_b (because of ion channels in the basal membrane) can result in high gain because of a reduction in the denominator in Eq. 6 as R_a neutralizes ($R_b + R_c$). The amplification role of the ampullary receptors also explains the requirement of two functional voltage-sensitive membranes (apical and basal membranes) in series instead of a single conducting membrane. Based on Figs.5–7, an ampullary organ is linear in its operational range ($\leq$100 μV). Apparently, the ampulla operates in this range as a linear amplifier (Fig. 10) with gain (gain factor is $R_b/(R_a + R_b + R_c)$). Further, if the amplification occurs with low background noise in this primary stage of signal processing, enhanced sensitivity could be achieved.

We thank Dr. A. J. Kalmijn for discussions and Drs. Richard Murphey, Todd L. Krause, and Harold Zakon for comments on the manuscript. We thank the Director of the Marine Biological Laboratory for the use of facilities.

This work was supported by Office of Naval Rerearch grant N00014-90-J-1137 (H. M. Fishman).

REFERENCES

Bennett, M. V. L., and W. T. Clusin. 1978. Physiology of the ampulla of Lorenzini, the electroreceptor of the elasmobranchs. *In* Sensor Biology of Sharks, Skates, and Rays. E. S. Hodgson and R. F. Mathewson, editors. U. S. Government Printing Office. 483–505.

Broun, G. R., and V. I. Govardovskii. 1983a. Electroreceptor mechanisms of the ampullae of Lorenzini in skates. *Neirofiziologiya.* 15:178–185.

Broun, G. R., and V. I. Govardovskii. 1983b. Electrical model of the electroreceptor of the ampulla of Lorenzini. *Neirofiziologiya.* 15:235–241.

Broun, G. R., V. I. Govardovskii, and V. L. Cherepnov. 1984. Effects of calcium, and potassium channel blockers on changes in transepithelial potential, and spike responses in Lorenzini ampullary electroreceptors in *Raja clavata. Neirofiziologiya.* 17:652–659.

Clusin, W. T., and M. V. L. Bennett. 1977a. Calcium-activated conductance in skate electroreceptors. Current clamp experiments. *J. Gen. Physiol.* 69:121.

Clusin, W. T., and M. V. L. Bennett. 1977b. Calcium-activated conductance in skate electroreceptors. Voltage clamp experiments. *J. Gen. Physiol.* 69:145.

Clusin, W. T., and M. V. L. Bennett. 1979. The oscillatory responses of skate electroreceptors to small voltage stimuli. *J. Gen. Physiol.* 73:685.

Cole, K. S. 1968. Test of the Hodgkin-Huxley axon. *In* Membranes, Ions and Impulses. K. S. Cole, editor. University of California Press, Berkeley, CA. 292–362.

Fishman, H. M. 1992. Assessment of conduction properties and thermal noise in cell membranes by admittance spectroscopy. *Bioelectromagnetics Suppl.* 1:87–100.

Fishman, H. M., and R. J. Lipicky. 1991. Determination of K^+-channel relaxation times in squid axon membrane by Hodgkin-Huxley and by direct linear analysis. *Biophys. Chem.* 39:177–190.

Fishman, H. M., and R. I. Macey. 1969. The N-shaped current-potential characteristic in frog skin. *Biophys. J.* 9:127–139.

Kalmijn, A. J. 1966. Electroreception in sharks and rays. *Nature.* 212: 1232–1233.

Kalmijn, A. J. 1982. Electric and magnetic field detection in elasmobranch fishes. *Science.* 218:916–918.

Mauro, A., F. Conti, F. Dodge, and R. Schor. 1970. Subthreshold behavior and phenomenological impedance of the squid giant axon. *J. Gen. Physiol.* 55:497–523.

Moore, L. E., H. M. Fishman, and D. J. M. Poussart. 1980. Small- signal analysis of K^+ conduction in squid axons. *J. Membr. Biol.* 54:157–164.

Murray, R. W. 1962. The response of the ampullae of Lorenzini of elasmobranches to electrical stimulation. *J. Exp. Biol.* 39:119.

Murray, R. W. 1967. The function of the ampullae of lorenzini of Elasmobranchs. *In* Lateral Line Detectors. P. Cahn, editor. Indiana University Press. 277–293.

Murray, R. W. 1974. The ampullae of Lorenzini. *In* Handbook of Sensory Physiology. Vol. 3. A. Fessard, editor. Springer-Verlag, Berlin. 125–145.

Obara, S., and M. V. L. Bennett. 1972. Mode of operation of ampullae of Lorenzini of the skate, Raja. *J. Gen. Physiol.* 60:534.

Waltman, B. 1966. Electrical properties and fine structure of the ampullary canals of Lorenzini. *Acta Physiol. Scand. Suppl.* 264:1–60.